Statistical Approach to the Corrosion Behavior of Dissimilar Welds of A387-Gr91/AISI316 Steels with PCGTAW Process

Mohammad Jula[1], Reza Dehmolaei[2,*], Seyed Reza Alavi Zaree[2]

[1]M Sc. student, Department of Material Science and Engineering, Shahid Chamran University of Ahvaz, Ahvaz, Iran
[2]Department of Material Science and Engineering, Shahid Chamran University of Ahvaz, Ahvaz, Iran

ARTICLE INFO

Article history:

Received 5 December 2016
Accepted 19 December 2016
Available online 15 March 2017

Keywords:

Taguchi method
Analysis of variance (ANOVA)
Pulsed current gas tungsten arc welding (PCGTAW)
Dissimilar welding
A387-Gr.91
AISI316

ABSTRACT

In this study, an attempt has been made to minimize the corrosion rate and maximize the pitting potential of dissimilar metal welded joints of A387-Gr91/AISI316 steels. The process parameters of the pulsed current gas tungsten arc welding (PCGTAW) including the peak current (P), background current (B), pulse frequency (F), and on time percentage (O) were chosen as the factors influencing the corrosion behavior. Design of Experiments (DOE) was done using Taguchi's L9 (34) orthogonal array. The signal to noise (S/N) ratio analysis indicated that corrosion rate was affected by the peak current, frequency, on time percentage, and background current, whereas the pitting potential was mostly influenced by on time percentage, peak current, frequency, and background current, respectively. Optimum conditions of P, B, F, and O factors were found as 135A, 75A, 10Hz, 80% for corrosion rate and 120A, 60A, 6Hz, 60% for the pitting potential, respectively. Furthermore, analysis of variance (ANOVA) demonstrated that the contribution of P, B, F, and O was 28.79%, 13.06%, 28.63%, and 29.51% for corrosion rate and 13.97%, 2.79%, 12.20%, and 71.04% for the pitting potential, respectively. Results of the welded samples at optimum conditions showed good agreement with the predicted values for corrosion rate and the pitting potential.

1-Introduction

Boiler components, such as main steam piping and the header parts of boilers, are usually exposed to high thermal stresses. A387-Gr.91steel is one of the suitable candidates for the mentioned application that explores good creep and fatigue resistance [1]. In other words, due to high corrosion, oxidation and creep resistance of austenitic stainless steels, super-heater and re-heater parts are made of these alloys [1, 2].

The welding of these two dissimilar steels by different welding routes has been the subject of wide research. Usually, the shielded metal arc welding (SMAW) and gas tungsten arc welding (GTAW) processes are applied to weld these alloys. The major problem encountered with the using of austenitic stainless steels as filler metals is possible carbon migration from ferritic steel to the welding metal and brittleness of the weld especially in the service temperatures more than 315°C. Welding of parts like tubes in the boiler that are in contact with the sulfurous environment by nickel-base fillers such as ERNiCrMo-3 is one solution to overcome the problem [3, 4, 5].

* Corresponding author:
E-mail address: Dehmolaei@scu.ac.ir

GTAW process is one of the fusion welding routes used in dissimilar welding of ferritic steels to austenitic stainless steels. Because of solidification structure, mechanical properties and corrosion resistance of the welding metal decline and it is possible to be modified by using pulsed current in the arc welding process [6]. This method involves cycling of the welding current from a high level to a low one at a selected regular frequency. The high level of the peak current is generally selected to give adequate penetration and bead contour, while the low level of the background current is set at a level sufficient to maintain a stable arc [7, 8]. The peak current, background current, frequency and on time percentage showed the greatest impact on properties in PCGTAW [9].
Using a full factorial design will bring all possible combinations for a given set of factors on table. However, since most industrial experiments usually involve a significant number of factors, this method results in a large number of experiments. Taguchi constructed a special set of general design guidelines for factorial experiments that cover many applications. In this case, the orthogonal array method presented by Taguchi is one of the most effective ways to reduce the number of experiments [10].
In the current research, the PCGTAW process parameters including the peak current, background current, frequency and on time percentage on three levels were changed and optimization of parameters to achieve the highest uniform and pitting corrosion resistance was done by using Taguchi's L_9 (3^4) orthogonal array.

2-Experimental Procedure

Chemical composition of AISI316 and A387-Gr.91 steels as base metals and ERNiCrMo-3 as filler metal are given in Table 1.
Specimens of 100×60×6 mm in size were cut from the as-received plates and standard V-groove butt joints with an included angle of 70 and a root face of 2 mm were prepared. Schematic of the joint design is presented in Figure 1.

Table1. Chemical composition of the base and filler metals.

Element (Wt.%)	Fe	Ni	Cr	Mn	Mo	V	Nb	Ti	Si	C
A387-Gr91	88.3	0.28	9.18	0.41	0.85	0.22	0.08	-	0.30	0.10
AISI316	70.4	10.2	16.5	1.52	2.61	0.08	-	0.03	0.72	0.05
ERNiCrMo-3	0.4	64	21.7	0.1	8.5	-	3.6	0.17	0.14	0.02

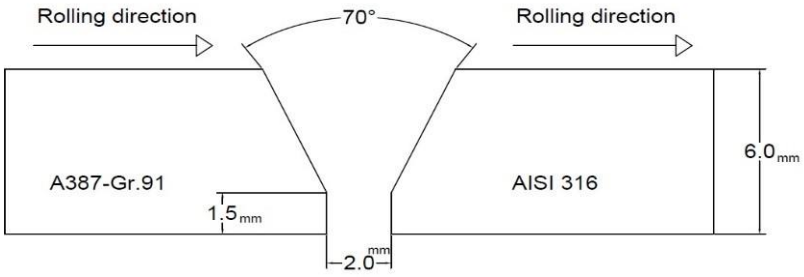

Fig. 1. Schematic of the joint design.

The PCGTAW route with tungsten electrode of 2% thorium and shielding gas (argon) flow rate of 15 L/min and 2.4 mm rod of ERNiCrMo-3 as filler metal was employed and three passes of welding were applied. Argon gas as the purge gas was injected with a flow rate of 10 L/min in the first and second passes. To avoid the cold cracking of A387-Gr.91 steel, the samples were preheated up to 275°C. Moreover, the maximum inter-pass temperature of 300°C was considered [11].
The main parameters of PCGTAW including the peak current, background current, frequency and on time percentage were altered at three different levels are listed in Table 2.

Table 2. PCGTAW process parameters and their levels.

	Peak current, A	Background current, A	Frequency, Hz	On time %
Code	A	B	C	D
Level1	120	60	2	40
Level2	135	75	6	60
Level3	150	90	10	80

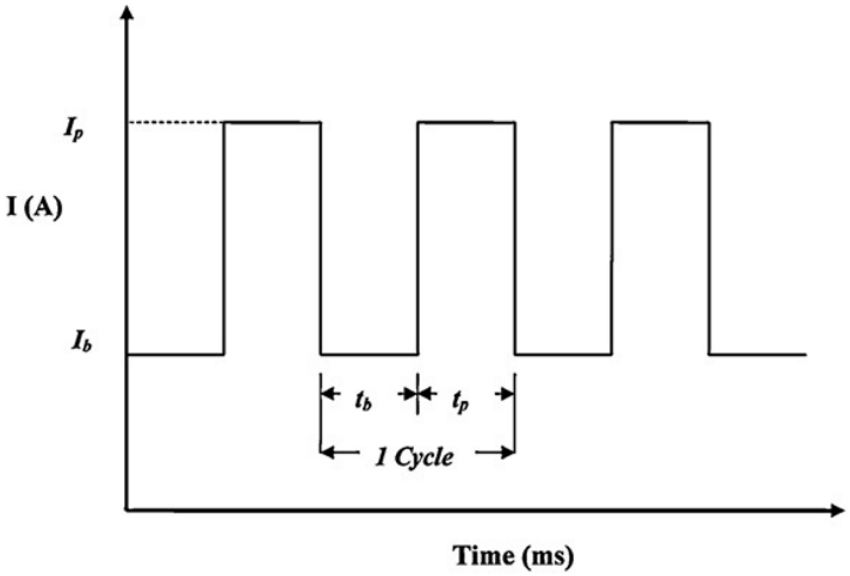

Fig. 2. Current-time chart. I_p is the peak current (A), I_b is the background current (A), t_p is the peak current duration (ms), and t_b is the background current duration (ms) [12].

According to Figure 2, the relations related to the frequency and on time percentage are presented in equations 1 and 2 [13].

$$f = 1/t_{cycle} = 1/t_p + t_b \quad (1)$$

$$\text{on time}\% = (t_p/t_p + t_b) \times 100 \quad (2)$$

Design of experiments (DOE) was done using Taguchi's L_9 (3^4) orthogonal array to investigate the effect of different levels of welding parameters and to obtain the optimal value for each parameter. This approach uses all the design factors with a minimum number of experiments [14,15]. As it is shown in Table 3, 9 experiments were conducted and each experiment was based on the combination of level values as shown in the table. The uniform corrosion resistance of the specimens was determined by polarization test method in accordance with the ASTM G3-89 and ASTM G59-97 standards [17, 18]. Polarization test was done in one liter of H_2SO_4 1.0N, at a scan rate of 600 mV/h, in the range of -100 to +100 mV relative to the open circuit potential and at a temperature of 20°C. The specimens were immersed in the solution for 55 min before beginning the polarization test to stabilize the open circuit potential and determine its value. The uniform corrosion rate was calculated by Tafel slope and Nova 1.11 software. Also, the Image Tools software was used to determine the tested surface area.

The pitting resistance of the specimens was investigated by polarization test based on the ASTM G3-89 and ASTM G5-94 standards [17, 19]. In this case, the polarization test is done in one liter of solution 3.5 wt.% NaCl, at a scan rate of 600 mV/h, the potential range of -300 to +1300 mV and temperature of 50°C. Also, before starting the test, the specimens were left in the solution for 55 minutes to stabilize the open circuit potential. An electrochemical cell consisted of platinum as

auxiliary electrode, saturated calomel as reference electrode (SCE), and the samples taken from Fusion zone as working electrode were used for both types of polarization tests.

Table3. Design of experiments (DOE) for welding parameters in accordance with L_9 orthogonal array.

Trial No.	Peak current, A	Background current, A	Frequency, Hz	On time %
1	120	60	2	40
2	120	75	6	60
3	120	90	10	80
4	135	60	6	80
5	135	75	10	40
6	135	90	2	60
7	150	60	10	60
8	150	75	2	80
9	150	90	6	40

3-Results and Discussion

The polarization test results of different specimens are reported in Table 4. The effect of different levels on the corrosion rate and pitting potential is analyzed by using the signal to noise (S/N) ratio. Comparison between the corrosion rate and pitting potential results was done by using the amount of S/N for each level of each parameter. The optimum level was identified and confirmation test was conducted. The comparison between both results from confirmation test and predicted one was done and was analyzed by ANOVA.

3-1-Taguchi results

According to the Taguchi method, by using S/N ratio instead of the mean values, there are three terms related to the S/N ratios for optimization of conditions including higher-the-better, lower-the-better and nominal-the-best [20]. Then, the lowest corrosion rate and the highest pitting potential are defined as optimal level of the parameters. The following equations were used in calculating the related S/N and the results are listed in Table 4.

$$\frac{S}{N} = -10 \log y^2 \quad (3)$$

$$\frac{S}{N} = -10 \log_{10} \frac{1}{y^2} \quad (4)$$

Table4. Corrosion rate and the pitting potential.

Trial No.	Corrosion Rate, (mm/year)	S/N Ratio, (dB)	Pitting Potential, (V_{SCE})	S/N Ratio, (dB)
1	0.00226	52.92	0.95	-0.45
2	0.00045	66.94	1.05	0.42
3	0.00038	68.40	0.93	-0.68
4	0.00024	72.40	0.91	-0.82
5	0.00022	73.15	0.92	-0.72
6	0.00057	64.88	0.97	-0.26
7	0.00033	69.63	1.01	0.09
8	0.00085	61.41	0.84	-1.51
9	0.00508	45.88	0.94	-0.54

The mean S/N ratio for each level of individual parameters was calculated from the data in Table 4. The obtained results and Δ function (equation 5) of all parameters are presented in Table 5 [21].

$$\Delta=\left(\frac{S}{N}\right)_{Max}-\left(\frac{S}{N}\right)_{min} \quad (5)$$

To study the main effect of each parameter on the test output, the response graphs of different process parameters for uniform corrosion rate and pitting potential were plotted and shown in Figures 3 and 4, respectively.

According to Figure 3 and Table 4 (bold values), the lowest uniform corrosion rate was achieved at the optimum condition of $\mathbf{A_2B_2C_3D_3}$. Figure 3 shows that by increasing the frequency and on time percentage, the uniform corrosion resistance was improved. According to Δ values in Table 4, the highest impact on the uniform corrosion rate belonged to the peak current, frequency, on time percentage and the background current, respectively.

On the other hand, the highest pitting potential occurred at optimum condition of $\mathbf{A_1B_1C_2D_2}$. Figure 4 shows that the pitting corrosion resistance is steadily reduced by increasing the maximum current and that a high level of on time percentage (80%) has a detrimental effect on the pitting resistance. According to the Δ values in Table 4, the on time parentage had the greatest impact on pitting potential. The effect of maximum current, frequency and background current on the pitting potential decreased respectively.

Table 5. S/N ratio response for the corrosion rate and pitting potential.

Parameters	Code	Level 1		Level 2		Level 3		Δ		Rank	
		Cor. Rate	E_{Pit}	Cor. Rate	E_{Pit}	Cor. Rate	E_{Pit}	Cor. Rate	E_{Pit}	Cor. Rate	E_{Pit}
Peak current	A	62.75	**-0.22**	**70.14**	-0.60	58.97	-0.66	11.17	0.43	1	2
Background current	B	64.98	**-0.39**	**67.17**	-0.60	59.72	-0.48	7.44	0.21	4	4
Frequency	C	59.74	-0.74	61.74	**-0.31**	**70.40**	-0.43	10.66	0.42	2	3
On time%	D	57.32	-0.57	67.15	**0.08**	**67.40**	-0.99	10.09	1.08	3	1

Note: The corrosion rate and pitting potential unit is (mm/year) and (V_{SCE}), respectively.

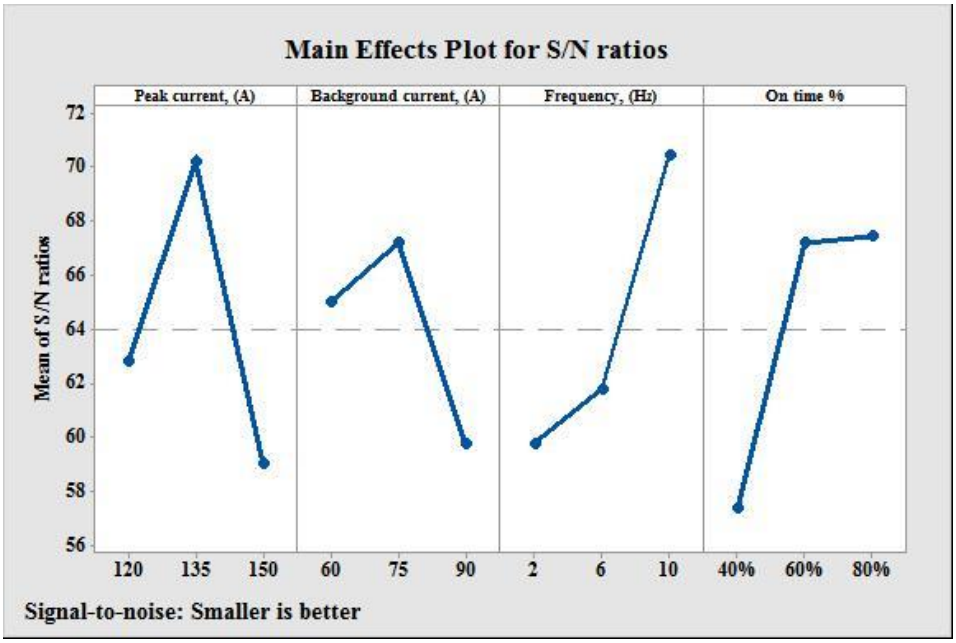

Fig. 3. S/N Response graph for corrosion rate.

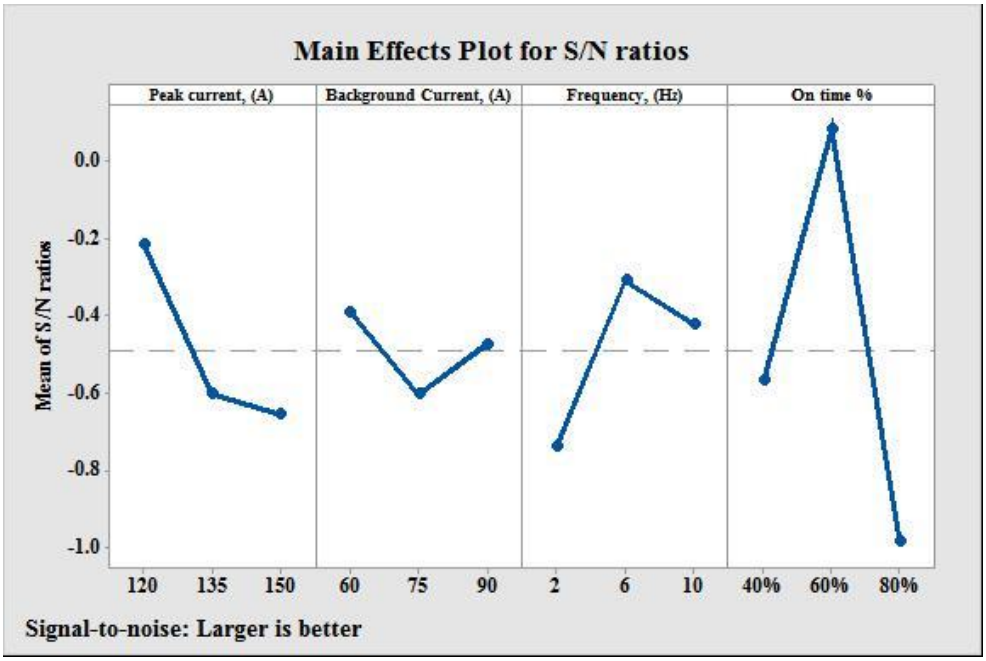

Fig. 4. S/N response graph for pitting potential.

3-2-Analysis of Variance (ANOVA) results

ANOVA was used to determine the influence of different factors. The sum of square (SS), the degrees of freedom (D), the variance (V) and the percentage of contribution to the total variation (P) are used in ANOVA, which can be calculated from the following equations [14, 20].

$$SS_T = \sum_{i=1}^{m} \eta_i^2 - \frac{1}{m}\left[\sum_{i=1}^{m} \eta_i\right]^2 \quad (6)$$

Where SS_T is the total sum of squares, m is the total number of experiments, and ηi is the S/N ratio at the *i*th test.

$$SS_P = \sum_{j=1}^{t} \frac{(S_{\eta j})^2}{t} - \frac{1}{m}\left[\sum_{i=1}^{m} \eta_i\right]^2 \quad (7)$$

where SS_p represents the sum of squares from the test factors, P represents one of the test factors, j the level number of this specific factor P, t the repetition of each level of factor P, and $S_{\eta j}$ the sum of the S/N ratio involving this factor and level j.

$$V_P\% = \frac{SS_P}{D_P} \times 100 \quad (8)$$

where V_P is the variance from the test factors, and D_P is the degree of freedom for each factor. The degrees of freedom (DOF) for the orthogonal array should be greater than or at least equal to those for the parameters. For example, a five-level design parameter accounts for four DOF. In this study, experimental DOF is 8 (number of trails minus one); while parameters-DOF is 2 (number of parameter levels minus one).

$$SS'_P = SS_P - D_P V_e \quad (9)$$

where SS'_p represents the corrected sum of squares from the tested factors and V_e denotes the variance for the error.

$$P_P = \frac{SS_P}{SS_T} \times 100 \quad (10)$$

where P_P is the percentage of the contribution to the total variation of each individual factor. The percentage contributions of each factor based on the corrosion rate and pitting potential obtained by the ANOVA results are illustrated in Tables 6 and 7, respectively. In addition, the influence of the PCGTAW process parameters on corrosion behaviors of weld metal is shown in Fig 5. According to the data in Tables 6 and 7 and the charts in Fig 5, it is clear that the highest on time percentage has the greatest impact on the uniform corrosion rate and pitting potential and after that the maximum effects are associated with maximum current, frequency and background current respectively. It is noteworthy that based on the results of the ANOVA the order of the effectiveness of parameters on the corrosion rate and pitting potential is similar. Another point to be noted is the mismatch between ranking the effect of various parameters on the uniform corrosion rate based on the Δ function in Taguchi results and contribution in the ANOVA results.

Table 6. Results of the S/N ratio ANOVA for the corrosion rate.

Character	Parameters	Degree of Freedom(D)	Sum of Squares(SS)	Variance(V)	Corrected Sum of Squares(SS´)	Contribution (P,%)	Rank	Significant
A	Peak Current	2	193.63	96.82	193.63	28.79	2	Yes
B	Background Current	2	87.82	43.91	87.82	13.06	4	Yes
C	Frequency	2	192.54	96.27	192.54	28.63	3	Yes
D	On time%	2	198.47	99.24	198.47	29.51	1	Yes
Error		0						
Total		8	672.46		672.46	100		

Table7. Results of the S/N ratio ANOVA for pitting potential.

Character	Parameters	Degree of Freedom(D)	Sum of Squares(SS)	Variance(V)	Corrected Sum of Squares(SS´)	Contribution (P,%)	Rank	Significant
A	Peak Current	2	0.34286	0.17143	0.34286	13.97	2	Yes
B	Background Current	2	0.06846	0.03423	0.06846	2.79	4	No
C	Frequency	2	0.29950	0.14975	0.29950	12.20	3	Yes
D	On time%	2	1.74382	0.87191	1.74382	71.04	1	Yes
Error		0						
Total		8	2.45464		2.45464	100		

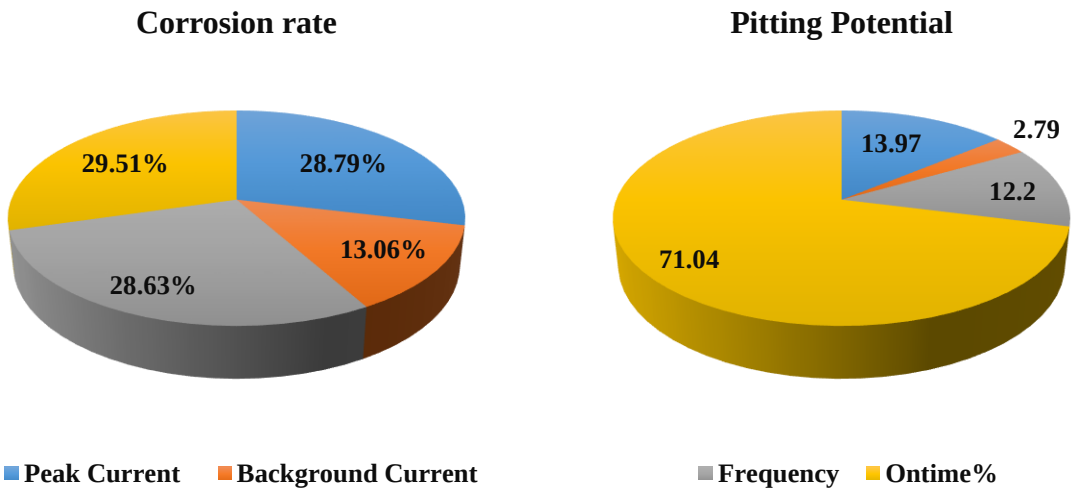

Fig. 5. Influence of PCGTAW process parameters on corrosion behaviors of weld metal obtained from S/N ratio ANOVA.

3-2-1-Pooled ANOVA

When the contribution of a factor is small, the sum of squares for that factor is combined with the error. This process of disregarding the contribution of a selected factor and subsequently adjusting the contributions of the other factor is known as pooling [22]. The results of ANOVA after pooling for the pitting potential are presented in Table 8. Also, the comparison chart of PCGTAW process parameters for the pitting potential is illustrated in Fig6.

Table8. Pooled ANOVA for the pitting potential.

Character	Parameters	Degree of Freedom(D)	Sum of Squares(SS)	Variance(V)	Corrected Sum of Squares(SS´)	Contribution (P,%)	Rank	Significant
A	Peak Current	2	0.34286	0.17143	0.27440	11.18	2	Yes
B	Background Current	(2)	(0.06846)	pooled				
C	Frequency	2	0.29950	0.14975	0.23104	9.41	3	Yes
D	on time%	2	1.74382	0.87191	1.67536	68.25	1	Yes
Error		2	0.06846	0.03423	0.27384	11.16		
Total		8	2.45464		2.45464	100		

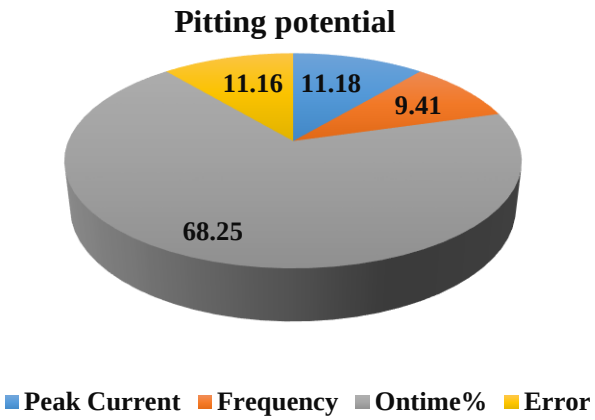

Fig. 6. Influence of PCGTAW process parameters on pitting potential of weld metal and error obtained from pooled ANOVA.

As can be seen in Figure 6, the background current is excluded from the analysis as the insignificant parameter and its effect is added to the error. Accordingly, the on time percentage, peak current and frequency with contributions 68.25%, 11.18% and 9.41% have the highest impact on the pitting potential. Also, the error percentage is 11.16.

The error variance shows the S/N differences per trial number within the same level for each factor [15].

3-3-Confirmation

As it was mentioned in Section 3.1, the optimum conditions for uniform corrosion rate and pitting potential are $\mathbf{A_2B_2C_3D_3}$ and $\mathbf{A_1B_1C_2D_2}$. So, two specimens are welded based on these conditions and the proper polarization tests were performed on them. The S/N ratio of the optimum specimen was determined based on Equation 11 [23].

$$\left[\frac{S}{N}\right]_{estimated} = \left[\frac{S}{N}\right]_M + \sum_{i=1}^{n}\left(\left[\frac{S}{N}\right]_i - \left[\frac{S}{N}\right]_M\right) \quad (11)$$

Where $[S/N]_M$ is the total mean S/N ratio, $[S/N]_i$ is the mean S/N ratio at the optimal level, and n is the number of parameters.

Table 9. Confirmation testing to validate the approach.

	Parameters								S/N ratio				Performance values			
	A: Peak Current, A		B:Background Current, A		C:Frequency Hz		D:on time%		Estimation		Experiment		Estimation		Experiment	
	Cor. Rate	E_{Pit}	Cor. Rate	E_{Pit}	Cor. Rate	E_{Pit}	Cor. Rate	E_{Pit}	Cor. Rate	E_{Pit}	Cor. Rate	E_{Pit}	Cor. Rate	E_{Pit}	Cor.Rate	E_{Pit}
Optimum level	2	1	2	1	3	2	3	2	83.24	0.64	80.92	0.75	0.00007	1.08	0.00009	1.09
Optimum value	135	120	75	60	10	6	80	60								

Note: The corrosion rate and pitting potential unit is (mm/year) and (V_{SCE}), respectively.

Table 9 shows the comparison of the predicted corrosion rate and the pitting potential with the experimental results using the optimal conditions. There is a good agreement between the predicted and the experimental results.

4-Conclusions:

The influence of pulsed current gas Tungsten arc welding process parameters such as the peak current, background current, frequency, and on time percentage on the corrosion behavior such as corrosion rate and pitting potential of A387-Gr91 to AISI316 alloys weld metals was studied and the main conclusions are summarized as follows:

- According to the results of S/N ratio and based on the values of Δ function, peak current, frequency, on time percentage and background current had the highest impact on the rate of uniform corrosion, respectively. Also, the on time percentage had the greatest impact on the pitting potential and then the greatest impacts are associated with maximum current, frequency and background current, respectively.
- According to the results of ANOVA, the effectiveness of parameters on the uniform corrosion rate and the pitting potential was similar; however, their contribution was different. The greatest impact on the uniform corrosion rate and pitting potential was associated with on time percentage, maximum current, frequency and background current, respectively.
- ANOVA results showed that the minimum effectiveness was associated with background current and this parameter was insignificant in the case of pitting potential. Pooled ANOVA table indicated that the contributions of on time percentage, peak current and frequency were 68.25%, 11.18% and 9.41%, respectively, and the error percentage was 11.16.
- Based on the results of S/N ratio, $\mathbf{A_2B_2C_3D_3}$ and $\mathbf{A_1B_1C_2D_2}$ were chosen as optimum conditions for uniform corrosion rate and pitting potential, respectively. Results from confirmation tests on the welded specimen were consistent with the predicted results based on the S/N ratio. The results of optimal specimens showed a significant improvement in corrosion resistance compared to other specimens.

References:

[1] F. Abe, T.U. Kern, R. Viswanathan, "Creep-Resistant Steels", Woodhead Publishing Limited and CRC Press, First Published, 2008

[2] M. Yamazaki, T. Watanabe, H. Hongo, M. Tabuchi, "Creep Rupture Properties of Welded Joints of Heat Resistant Steels", International Conference on Power Engineering, 2007, pp. 1044-1048

[3] A.K. Bhaduri, S. Venkadesan, P. Rodriguez, " Transition metal joints for steam generators-An overview", Int. J. Pres. Ves. Pip., Vol. 58,1994, pp. 251-265

[4] Y.Y. You, R.K. Shiue, "the Study of Carbon Migration in Dissimilar Welding of the Modified 9Cr-1Mo Steel", J. Mater. Sci. Lett., Vol. 20, 2001, pp. 1429-1432

[5] American Petroleum Institude, "Welding Guidelines for the Chemical, Oil, and Gas Industries", Recommended Practice 582, 2001
[6] K.D. Ramakumar, S. Oza, S. Periwal, N. Arivazhagan, R. Sridhar, S. Narayanan, "Characterization of Weld Strength and Toughness in the Multi-Pass Welding of Inconel625 and Super Duplex Stainless Steel UNS32750", Cienc. Tec. Mater., Vol. 27, 2015, pp. 41-52
[7] A. Hadadzadeh, M.M. Ghaznavi, A.H. Kokabi, "The Effect of Gas Tungsten Arc Welding and Pulsed-Gas Tungsten Arc Welding Processes' Parameters on The Heat Affected Zone-Softening Behavior of Strain-Hardened Al–6.7Mg Alloy", Mater. Des., Vol. 55, 2014, pp. 335-342
[8] H.G. Fan, Y.W. Shi, S.J. Na, "Numerical Analysis of The Arc in Pulsed Current Gas Tungsten Arc Welding Using a Boundary-Fitted Coordinate", J. Mater. Process. Technol., Vol. 72, 1997, pp. 437-445
[9] T.S. kumar, V. Balasubramanian, M.Y. Sanavullah, " Influences of Pulsed Current Tungsten Inert Gas Welding Parameters on The Tensile Properties of AA 6061 Aluminum Alloy", Mater. Des., Vol. 28, 2007, pp. 2080-2092
[10] J. Antony, M. Kaye, "Experimental Quality: A Strategic Approach to Achieve and Improve Quality", Springer, 2000
[11] American Society of Mechanical Engineers, "Qualification Standard for Welding and Brazing Procedures, Welders, Brazers, and Welding and Brazing Operators", Boiler and Pressure Vessel Code Sec. IX, 2010
[12] M. Yousefieh, M. Shamanian, A. Saatchi, "Optimization of the Pulsed Current Gas Tungsten Arc Welding (PCGTAW) Parameters for Corrosion Resistance of Super Duplex Stainless Steel Parameters for Corrosion Resistance of Super Duplex Stainless Steel", J. Alloys Compd., Vol. 509, 2011, pp. 782-788
[13] Z. Tong, Z. Zhenati, Z. Rui, "A dynamic welding heat source model in pulsed current gas tungsten arc welding", J. Mater. Process. Technol., Vol. 213, 2013, pp. 2329-2338
[14] M. Manikandan, M.N. Rao, R. Ramanujam, D. Ramakumar, N. Arivazhagan, G.M. Reddy, "Optimization of The Pulsed Current Gas Tungsten Arc Welding Process Parameters for Alloy C-276 Using the Taguchi Method", Procedia Eng., Vol. 97, 2014, pp. 767-774
[15] G. Taguchi, S. Chowdhury, Y. Wu, "Taguchi's Quality Engineering Handbook", John Wiley & Sons, 2005
[16] M. Arivarasu, K.D. Ramakumar, N. Arivazhagan, "Comparative Studies of High and Low Frequency Pulsing On the Aspect Ratio of Weld Bead in Gas Tungsten Arc Welded AISI 304L Plates", Procedia Eng., Vol. 97, 2014, pp. 871-880
[17] American Society for Testing and Materials, "Standard Practice for Conventions Applicable to Electrochemical Measurements in Corrosion Testing", ASTM G3-89, 1999
[18] American Society for Testing and Materials, "Standard Test Method for Conducting Potentiodynamic Polarization Resistance Measurements", ASTM G59-97, 2003
[19] American Society for Testing and Materials, "Standard Reference Test Method for Making Potentiostatic and Potentiodynamic Anodic Polarization Measurements", ASTM G5-94, 1999
[20] M. Yousefieh, M. Shamanian, A. Saatchi, "Optimization of Experimental Conditions of the Pulsed Current GTAW Parameters for Mechanical Properties of SDSS UNS S32760 Welds Based on the Taguchi Design Method", J. Mater. Eng. Perform., Vol. 21(9), 2012, pp. 1978-1988
[21] M. Yousefieh, M. Shamanian, A. R. Arghavan, "Analysis of Design of Experiments Methodology for Optimization of Pulsed Current GTAW Process Parameters for Ultimate Tensile Strength of UNS S32760 Welds", Metallogr. Microstruct. Anal., Vol. 1, 2012, pp. 85-91
[22] R. K. Roy, "A Primer on The Taguchi Method", Society of Manufacturing Engineers, Second Edition, 2010
[23] E. Rastkerdar, M. Shamanian, A. Saatchi, "Taguchi Optimization of Pulsed Current GTA Welding Parameters for Improved Corrosion Resistance of 5083 Aluminum Welds", J. Mater. Eng. Perform., Vol. 22, 2013, pp. 1149-1160